Radio Science, Volume 22, Number 6, Pages 1053–1062, November 1987

An improved prediction method for rain attenuation in satellite communications operating at 10–20 GHz

M. Yamada, Y. Karasawa, and M. Yasunaga

Research and Development Laboratories, KDD, Tokyo, Japan

B. Arbesser-Rastburg

Antennas and Propagation, R & D, INTELSAT, Washington D. C.

(Received April 28, 1987; revised July 15, 1987; accepted July 17, 1987.)

Several prediction methods for rain attenuation presented so far are evaluated using a common long-term data base (total 124 sets of measurements) for oblique propagation paths with frequencies of from 10 to 20 GHz, and an improved prediction method reflecting the evaluation results performed is proposed. The evaluation results indicate that CCIR methods give relatively high precision, although in this respect, there is not such a great difference from other methods. The method proposed here includes a rain area size parameter as a function of rain rate for 0.01% of the time so as to minimize the prediction error. It is verified that the method thus obtained gives the best precision, at the present time, for predicting rain attenuation on Earth-to-space propagation paths at 10–20 GHz.

1. INTRODUCTION

In order to cope with increased demand in international satellite communications by INTELSAT, the use of the 14/11 GHz and 14/12 GHz frequency bands is being introduced in addition to the existing 6/4 GHz band. At frequencies above 10 GHz, however, the attenuation of signals due to rain is a serious problem in the design of communication systems. Therefore many researchers have focused their energies on establishing a reliable prediction method for rain attenuation.

Various types of prediction methods for rain attenuation have been discussed, mainly by the CCIR study group 5, for a considerable time, improvements to the prediction method being made at every meeting. In parallel to the work of the CCIR, some other methods have also been proposed independently. Under such circumstances, an evaluation of the prediction accuracy of these methods and an assessment of their limits of applicability based on a common data base are strongly required with a view to designing reliable satellite communication systems.

In this paper, we will describe the results of an evaluation of various prediction methods, including CCIR methods, using long-term data (total of 124 sets of measurements) reported so far for oblique propagation paths, and propose an improved prediction method reflecting the evaluation results performed.

Paper number 7S0621.
0048-6604/87/007S-0621$08.00

2. EVALUATION OF EXISTING PREDICTION METHODS

2.1. *Methods examined*

The evaluation is performed on following eight existing methods for which calculation procedures are described in detail: A-1, *CCIR Rep. 564-2 (MOD I)* [1984] (out of print); A-2, *CCIR Rep. 564-2 (MOD F)* [1986]; A-3, Crane's method (1) (global model) [*Crane*, 1980]; A-4, Crane's method (2) (two-component model) [*Crane*, 1985*a*]; A-5, Morita's method [*Morita*, 1980]; A-6, Misme and Waldteufel's method [*Misme and Waldteufel*, 1980]; A-7, Lin's method [*Lin*, 1979]; A-8, Stutzman and Dishman's method [*Stutzman and Dishman*, 1982].

2.2. *Evaluation procedure*

Data used for examination. To evaluate these prediction methods, 86 measurements registered in the CCIR data bank [*CCIR*, 1985] and another 38 measurements reported in other papers, are used.

TABLE 1. List of Data for Evaluation

Number	Location (Country)	Latitude	Station Height, m	Period	Climatic Zone	Method	Frequency, GHz	Elevation	Reference
1	Sodankyla (Finland)	67.4N	180	7901/8312	E	SAT	11.6	13.2	CCIR (316-1)
2	Marugame (Japan)	34.3N	10	7905/8004	M	RDM	11.9	45	CCIR (611-3)
3	Marugame (Japan)	34.3N	10	7905/8004	M	RDM	11.9	15.0	CCIR (611-2)
4	Lario (Italy)	46.2N	210	7801/8012	K	SAT	11.6	32	CCIR (313-1)
5	Spino d'Adda (Italy)	45.4N	80	7810/8009	K	SAT	11.6	32	CCIR (314-1)
6	Fucino (Italy)	42.0N	680	7801/8012	K	SAT	11.6	33	CCIR (315)
7	Austin, Tex. (U.S.)	30.4N	239	7606/7906	M	SAT	11.7	50	CCIR (110-1, 2, 3)
8	Waltham, Mass. (U.S.)	42.4N	50	7706/7905	K	SAT	11.7	24	CCIR (102-1, 2)
9	Holmdel (U.S.)	40.4N	115	7604/7704	K	SAT	11.7	27	*Rustako* [1978]
10	Leeheim (F. R. G.)	49.9N	90	7901/7912	E	SAT	11.6	28.8	*Rucker* [1980]
11	Leeheim (F. R. G.)	49.9N	90	7901/7912	E	SAT	11.6	32.5	*Rucker* [1980]
12	Leeheim (F. R. G.)	49.9N	90	7401/7612	E	RDM	11.4	32.5	*Rucker* [1980]
13	Slough (U.K.)	51.5N	30	7301/7512	G	RDM	11.6	29.5	*Allnutt* [1977]
14	Etam, W. Va. (U.S.)	39.3N	560	7710/7810	K	RDM	11.6	18	CCIR (113-1)
15	Lenox, W. Va. (U.S.)	39.6N	610	7710/7810	K	RDM	11.6	18	CCIR (112-1)
16	Kashima (Japan)	35.6N	40	7901/8112	K	SAT	11.7	37	CCIR (604-3)
17	Kashima (Japan)	35.6N	40	7705/7804	K	SAT	11.5	47	CCIR (604-1)
18	Innisfail (Australia)	17.6S	10	7412/7610	N	RDM	11.1	30	CCIR (703-1)
19	Innisfail (Australia)	17.6S	10	7611/7904	N	RDM	11.1	45	CCIR (703-2)
20	Darwin (Australia)	17.6S	20	7711/7904	N	RDM	11.0	60	CCIR (702-1)
21	Clarksburg, Md. (U.S.)	39.2N	180	7607/7707	K	RDM	11.6	21	CCIR (105-2)
22	Clarksburg, Md. (U.S.)	39.2N	180	7708/7808	K	RDM	11.6	41	CCIR (105-3)
23	Clarksburg, Md. (U.S.)	39.2N	180	7808/7908	K	RDM	11.6	43.5	CCIR (105-4)
24	Clarksburg, Md. (U.S.)	39.2N	180	7410/7509	K	RDM	11.6	42	CCIR (105-1)
25	Greenbelt (U.S.)	38.5N	200	7604/7704	K	SAT	11.7	29	CCIR (106-1)
26	Greenbelt (U.S.)	38.5N	200	7704/7804	K	SAT	11.7	29	CCIR (106-2)
27	Greenbelt (U.S.)	38.5N	200	7804/7904	K	SAT	11.7	29	CCIR (106-3)
28	Holmdel (U.S.)	40.39N	115	7606/7706	K	SAT	11.7	27	CCIR (104-1)
29	Holmdel (U.S.)	40.39N	115	7706/7806	K	SAT	11.7	27	CCIR (104-2)
30	Holmdel (U.S.)	40.39N	115	7806/7906	K	SAT	11.7	27	CCIR (104-3)
31	Munich (F. R. G.)	48.2N	510	7801/7812	K	SAT	11.6	29	*Rogers* [1979]
32	Harwell (U.K.)	51.6N		7511/7611	E	RDM	11.6	28	*Rogers and Hyde* [1978]
33	Boston, Mass. (U.S.)	42.4N		7505/7605	K	RDM	11.6	25	*Rogers and Hyde* [1978]
34	Singapore	1.3N	20	7601/7702	P	RDM	11.6	41	CCIR (622-1)
35	Hong Kong	22.3N	20	7512/7701	N	RDM	11.6	20	CCIR (623-1)
36	Michelbachberg (Austria)	47.5N		7605/7706	K	RDM	11.6	33	*Rogers and Hyde* [1978]
37	Bringelly (Australia)	33.9S		7601/7703	N	RDM	11.6	43	*Rogers and Hyde* [1978]
38	Martlesham (U.K.)	52.1N	30	7901/8112	E	SAT	11.8	29.9	CCIR (306-2)
39	Leeheim (F. R. G.)	49.9N	90	7901/8101	D	SAT	11.6	30	*Dintelman* [1983]
40	Gometz (France)	48.7N	170	7801/7812	H	SAT	11.6	32	CCIR (311-1)
41	Gometz (France)	48.7N	170	7901/7912	H	SAT	11.8	33.6	CCIR (311-3)
42	Bern (Switzerland)	47.0N	650	7401/7612	H	RDM	11.45	35	CCIR (311-3)
43	Fucino (Italy)	42.0N	650	7301/7412	K	RDM	11.45	42	CCIR (311-3)
44	Stockholm (Sweden)	59.0N	65	7301/7612	E	RDM	11.45	21	CCIR (311-3)
45	Milano (Italy)	45.8N	130	7301/7412	L	RDM	11.45	37	CCIR (311-3)
46	Porto (Portugal)	38.0N	1050	7401/7512	H	RDM	11.45	40	CCIR (311-3)
47	Buitrago (Spain)	40.5N	600	7401/7512	H	RDM	11.45	40	CCIR (311-3)
48	Graz (Austria)	47.3N	450	7401/7612	K	RDM	11.45	34	CCIR (311-3)
49	Marugame (Japan)	34.3N	10	7701/8009	M	RDM	11.9	6	*Yasukawa and Yamada* [1985]
50	Yamaguchi (Japan)	34.2N	121	7910/8009	M	RDM	11.9	9.2	*Yasukawa and Yamada* [1985]
51	Hamada (Japan)	34.9N	216	7910/8009	M	RDM	11.9	8.4	*Yasukawa and Yamada* [1985]
52	Shimotsui (Japan)	34.5N	35	7810/7909	K	RDM	11.9	6.0	*Yasukawa and Yamada* [1985]
53	Kurashiki (Japan)	34.6N	10	7810/7909	K	RDM	11.9	6.0	*Yasukawa and Yamada* [1985]
54	Blacksburg (U.S.)	37.2N	640	7701/7711	K	SAT	11.7	33	CCIR (108-1)

TABLE 1. (continued)

Number	Location (Country)	Latitude	Station Height, m	Period	Climatic Zone	Method	Frequency, GHz	Elevation	Reference
55	Blacksburg (U.S.)	37.2N	640	7801/7812	K	SAT	11.7	33	CCIR (108-2)
56	Blacksburg (U.S.)	37.2N	640	7606/7906	K	SAT	11.7	33	CCIR (108-3)
57	Blacksburg, Va. (U.S.)	32.7N	643	7901/8112	K	SAT	11.6	10.7	CCIR (108-7)
58	Albertslund (Denmark)	55.7N	30	7901/8112	E	SAT	11.8	26.5	CCIR (305-3)
59	Martlesham (U.K.)	52.1N	30	7901/8112	G	SAT	11.6	29.9	CCIR (306-1)
60	Nederhorst (Holland)	52.2N	20	7901/8112	E	SAT	11.6	30.0	CCIR (307-1)
61	Slough (U.K.)	51.5N	30	7807/8008	E	SAT	11.8	30.3	CCIR (308-1)
62	Slough (U.K.)	51.5N	30	7709/8008	E	SAT	11.6	29.5	CCIR (308-2)
63	Leeheim (F. R. G.)	49.9N	90	7901/7912	E	SAT	11.8	32.9	CCIR (309-2)
64	Leeheim (F. R. G.)	49.9N	90	8001/8012	E	SAT	11.8	32.9	CCIR (309-3)
65	Leeheim (F. R. G.)	49.9N	90	8101/8112	E	SAT	11.8	32.9	CCIR (309-4)
66	Gometz (France)	48.7N	170	7901/7912	H	SAT	11.6	32.0	CCIR (311-2)
67	Munich (F. R. G.)	48.2N	510	7901/7912	K	SAT	11.6	29.0	CCIR (312-1)
68	Kirkkonummi (Finland)	60.2N	60	7901/8012	E	SAT	11.8	20.6	CCIR (317-1)
69	Stockholm (Sweden)	59.3N	60	7901/7912	E	SAT	11.6	22.4	CCIR (318-2)
70	Lustbuehel (Austria)	47.1N	490	7901/8212	K	SAT	11.6	35.2	CCIR (319-1)
71	Lyngby (Denmark)	55.7N	30	8001/8112	E	SAT	11.8	26.5	CCIR (320-1)
72	Wakkanai (Japan)	45.3N	60	7809/7909	K	SAT	12.06	29	CCIR (601-1)
73	Kesennuma (Japan)	38.8N	10	7809/7909	K	SAT	12.06	34.4	CCIR (615-1)
74	Osaka (Japan)	34.7N	40	7809/7909	M	SAT	12.06	41.0	CCIR (610-1)
75	Owase (Japan)	34.3N	10	7809/7909	M	SAT	12.06	41.5	CCIR (613-1)
76	Matsue (Japan)	35.5N	20	7809/7909	M	SAT	12.06	42.0	CCIR (606-1)
77	Ogasawara (Japan)	27.1N	50	7809/7909	M	SAT	12.06	42.5	CCIR (617-1)
78	Ashizuri (Japan)	32.8N	100	7809/7909	M	SAT	12.06	44.6	CCIR (614-1)
79	Yamagawa (Japan)	31.2N	80	7809/7909	M	SAT	12.06	47.3	CCIR (616-1)
80	Minamidaito (Japan)	25.8N	190	7809/7909	N	SAT	12.06	51.7	CCIR (618-1)
81	Yonaguni (Japan)	24.5N	200	7809/7909	N	SAT	12.06	57.9	CCIR (620-1)
82	Austin, Tex. (U.S.)	30.4N	239	7810/8011	M	RDM	13.6	52	CCIR (110-4)
83	Palmetto, Ga. (U.S.)	33.3N	100	7306/7506	M	RDM	13.6	38.2	*Lin et al.* [1980]
84	Palmetto, Ga. (U.S.)	33.3N	100	7606/7707	M	RDM	13.6	29.9	*Lin et al.* [1980]
85	Palmetto, Ga. (U.S.)	33.3N	100	7708/7808	M	RDM	13.6	49.5	*Lin et al.* [1980]
86	Grant Park, Ill. (U.S.)	41.1N	100	7607/7707	K	RDM	13.6	27.3	*Lin et al.* [1980]
87	Grant Park, Ill. (U.S.)	41.1N	100	7708/7808	K	RDM	13.6	41.8	*Lin et al.* [1980]
88	Longmont, Colo. (U.S.)	40.N	1500	7306/7506	E	RDM	13.6	42.6	*Lin et al.* [1980]
89	Ibaraki (Japan)	34.1N	57	7506/8005	K	RDR	13.85	10	*Yamada et al.* [1981]
90	Martlesham (U.K.)	52.1N	30	7901/8112	E	SAT	14.5	29.9	CCIR (306-3)
91	Albertslund (Denmark)	55.7N	30	7901/8112	E	SAT	14.5	26.5	CCIR (305-4)
92	Gometz (France)	48.7N	170	7901/7912	H	SAT	14.5	33.6	CCIR (311-4)
93	Stockholm (Sweden)	59.3N	60	7901/7912	E	SAT	14.5	22.4	CCIR (318-3)
94	Holmdel (U.S.)	40.4N	150	6909/7109	K	RDM	15.5	32	*Lin et al.* [1980]
95	Holmdel (U.S.)	40.4N	150	7111/7211	K	RDM	15.5	32	*Lin et al.* [1980]
96	Holmdel (U.S.)	40.4N	150	7001/7012	K	RDM	16.0	32.0	*Wilson and Mammel* [1973]
97	Palmetto, Ga. (U.S.)	33.3N	290	7306/7506	M	RDM	17.8	38.2	*Lin et al.* [1980]
98	Palmetto, Ga. (U.S.)	33.3N	290	7606/7706	M	RDM	17.8	29.9	*Lin et al.* [1980]
99	Longmont, Colo. (U.S.)	40N	1500	7306/7506	E	RDM	17.8	42.6	*Lin et al.* [1980]
100	Lario (Italy)	46.2N	210	7801/8112	K	SAT	17.8	32.0	CCIR (313-2)
101	Fucino (Italy)	42.0N	680	7801/8112	K	SAT	17.8	31.0	CCIR (315-2)
102	Kawasaki (Japan)	35.5N	20	7503/7605	K	RDM	18.0	20	*Satoh et. al.* [1978]
103	Kawasaki (Japan)	35.5N	20	7503/7605	K	RDM	18.0	55	*Satoh et. al.* [1978]
104	Holmdel (U.S.)	40.4N	110	7607/7806	K	SAT	19.0	18.5	CCIR (104-4)
105	Holmdel (U.S.)	40.4N	110	7705/7805	K	SAT	19.0	38.6	CCIR (104-5, 6)
106	Tampa (U.S.)	27.6N	20	7901/7912	N	SAT	19.0	57.0	CCIR (111-1)
107	Austin, Tex. (U.S.)	30.4N	239	7810/808	M	SAT	19.0	52	CCIR (110-5)
108	Palmetto, Ga. (U.S.)	33.3N	100	7606/7707	M	SAT	19.0	29.9	CCIR (109-1)

TABLE 1. (continued)

Number	Location (Country)	Latitude	Station Height, m	Period	Climatic Zone	Method	Frequency, GHz	Elevation	Reference
109	Palmetto, Ga. (U.S.)	33.3N	100	7708/7808	M	SAT	19.0	49.5	CCIR (109-2)
110	Grant Park, Ill. (U.S.)	41.4N	100	7607/7706	K	SAT	19.0	27.3	CCIR (103-1)
111	Grant Park, Ill. (U.S.)	41.4N	100	7708/7808	K	SAT	19.0	41.8	CCIR (103-2)
112	Blacksburg, Va. (U.S.)	37.2N	640	7707/8008	K	SAT	19.0	45	CCIR (108-10)
113	Blacksburg, Va. (U.S.)	37.2N	640	7707/8008	K	SAT	19.0	45	CCIR (108-11)
114	Clarksburg, Md. (U.S.)	39.2N	180	7607/7707	K	SAT	19.0	21	CCIR (105-5)
115	Clarksburg, Md. (U.S.)	39.2N	180	7607/7707	K	SAT	19.0	21	CCIR (105-6)
116	Clarksburg, Md. (U.S.)	39.2N	180	7708/7808	K	SAT	19.0	41	CCIR (105-7)
117	Clarksburg, Md. (U.S.)	39.2N	180	7708/7808	K	SAT	19.0	41	CCIR (105-8)
118	Clarksburg, Md. (U.S.)	39.2N	180	7808/8009	K	SAT	19.0	43.5	CCIR (105-9)
119	Kashima (Japan)	35.6N	40	7804/8203	K	SAT	19.45	48	CCIR (604-4)
120	Waltham (U.S.)	42.4N	10	7901/7912	K	SAT	19.0	38.5	CCIR (102-4)
121	Waltham (U.S.)	42.4N	10	7801/7812	K	SAT	19.0	35.6	CCIR (102-3)
122	Tampa (U.S.)	27.6N	10	7901/7912	N	SAT	19.0	54.5	CCIR (111-2)
123	Yokosuka (Japan)	35.1N	110	7804/7903	M	SAT	19.45	48.0	CCIR (608-1)
124	Yokohama (Japan)	35.2N	20	7804/7903	K	SAT	19.45	48.0	CCIR (607-1)

These data are limited to oblique propagation paths at frequencies of 10 GHz to 20 GHz. In these measurements, 77 are from measurements using satellites (SAT), 46 using a radiometer (RDM), and 1 using radar (RDR). The configuration of each measurement is summarized in Table 1.

For evaluation, the following procedure is adopted: data obtained over a period of 10 months or more are selected for examination. Weighting factors are assigned as follows: 10–21 months, 1; 22–33 months, 2; 34–45 months, 3; more than 46 months, 4.

Observations taken at the same point, but at different frequencies and elevations, are treated as independent data.

Rain rate. Every method requires the intensity of rainfall rate for certain percentages of the time for the computation of rain attenuation. In order to put the conditions on a common basis as far as possible, two types of evaluation are performed: (1) evaluation using assigned rain data from the CCIR rain-climatic zone [*CCIR Rep. 563*, 1982]; (2) evaluation using experimental rain rate data. In the case of Crane's two-component model (A-4), five parameters including the probability of the occurrence of strong rain (cell), and weak rain (debris), and the mean rainfall rate are necessary for calculations, and these parameters cannot be obtained directly from the usual observations of rain intensity. Therefore only evaluation (1) is performed using the above parameters for each climatic zone assigned by *Crane* [1985*b*].

Measure of evaluation. For evaluating prediction accuracy, the mean error, $\overline{\Delta X}$ (%), and standard deviation, $\sigma_{\Delta x}$ (%), are used. These parameters are defined as follows:

$$\overline{\Delta X} = \frac{1}{\sum_{i=1}^{N} W_i} \sum_{i=1}^{N} \left\{ \frac{W_i(X_{pi} - X_{mi})}{X_{mi}} \right\} \times 100\ (\%)$$

$$\sigma_{\Delta X} = \left\{ \frac{1}{\sum_{i=1}^{N}} \sum_{i=1}^{N} W_i \left(\frac{X_{pi} - X_{mi}}{X_{mi}} - \frac{\overline{\Delta X}}{100} \right)^2 \right\}^{1/2} \times 100\ (\%)$$

where

X_{pi} predicted attenuation for the ith measurement;
X_{mi} ith measured attenuation;
W_i weighting function of the ith measurement;
N total number of sets of data.

2.3. *Results of evaluation*

Prediction discrepancies are evaluated in the following four cases with different conditions for fraction of times of 0.001%, 0.01%, 0.1%, and 1%.

Case 1. All data in the frequency range 10–15 GHz (93 measurements).

Case 2. Data in the frequency range 10–15 GHz at elevations of 20° or less (12 measurements).

Case 3. Data in the frequency range 10–15 GHz at elevations of above 20° (81 measurements).

TABLE 2*a*. Results of Evaluation for Existing Prediction Methods: Mean Errors

Case	Condition	Time Rate, %	CCIR MOD I (A-1), %	CCIR MOD F (A-2), %	Crane-G (A-3), %	Crane-2C (A-4), %	Morita (A-5), %	M & W (A-6), %	Lin (A-7), %	S & D (A-8), %
1-a	$f = 10$–15 GHz	1.	80	12*	−34	−20	14†	−20	−53	−49
	Rain rate:	0.1	7	13	1*	3	2	2	14	−1*
	CCIR zone	0.01	2*	6†	24	15	10	10	49	16
		0.001	4*	7†	85	51	32	32	111	60
1-b	$f = 10$–15 GHz	1.	85	15*	−17†	···	33	−19	−35	−30
	Rain rate:	0.1	12†	18	−11*	···	71	12†	26	14
	measured	0.01	14*	19†	30	···	81	36	61	26
		0.001	8*	12†	57	···	135	92	71	38
2-a	$f = 10$–15 GHz	1.	77	7	−6†	−9	48	−1*	39	−34
	Rain rate:	0.1	2*	7	5	12	92	−2*	40	14
	CCIR zone	0.01	16*	22	24	46	124	16*	106	23
	$El \leq 20°$	0.001	46†	54	57	106	187	30*	149	57
2-b	$f = 10$–15 GHz	1.	67	2†	0*	···	50	−9	−31	−24
	Rain rate:	0.1	−2*	3†	11	···	96	11	46	24
	measured	0.01	37	44	36†	···	166	36†	130	35*
	$El \leq 20°$	0.001	···	···	···	···	···	···	···	···
3-a	$f = 10$–15 GHz	1.	83	15†	−57	−29	−14*	−36	−63	−61
	Rain rate:	0.1	9	16	−1*	−2†	32	4	2†	−8
	CCIR zone	0.01	−1*	3†	24	10	48	9	39	14
	$El > 20°$	0.001	−2*	4†	87	48	90	32	110	60
3-b	$f = 10$–15 GHz	1.	103	28†	−28†	···	17*	−31	−39	−34
	Rain rate:	0.1	21	28	11	···	50	9†	11	7*
	measured	0.01	8*	13†	29	···	53	36	44	24
	$El > 20°$	0.001	8*	12†	57	···	135	92	25	38
4-a	$f = 15$–20 GHz	1.0	133	42	−37	1*	−4†	−39	−44	−40
	Rain rate:	0.1	−3†	0*	−9	−10	8	−3†	−11	−18
	CCIR zone	0.01	−6	−3*	13	−3*	30	16	17	9
		0.001	21*	25†	82	50	133	92	65	73
4-b	$f = 15$–20 GHz	1.	148	47	−27	···	8*	−9†	−31	−27
	Rain rate:	0.1	16	18	−7†	···	26	16	−6*	−16
	measured	0.01	2*	6†	20	···	37	25	28	17
		0.001	−23†	−21*	58	···	95	84	40	49

*Best values.
†Second best values.

Case 4. All data in the frequency range 15–20 GHz (31 measurements).

It should be noted that for some cases a complete set of data was not available for each fraction of time, so the total number of data points for each fraction of time is less than the number of measurements stated above.

Table 2 shows the mean values $\overline{\Delta X}$ and standard deviations $\sigma_{\Delta X}$ obtained for each of the above prediction methods under each set of conditions cited above. The asterisks and daggers in the table, respectively, indicate the method which gives the most precise value (i.e., the smallest discrepancy), and the method which gives the second best value in a given fraction of time.

The following is evident from the table:

1. As for the mean value, the CCIR methods (A-1 and A-2) give better precision than the other methods. The other methods have no particular advantages or disadvantages.

TABLE 2*b*. Results of Evaluation for Existing Prediction Methods: Standard Deviations

Case	Condition	Time Rate, %	CCIR MOD I (A-1), %	CCIR MOD F (A-2), %	Crane-G (A-3), %	Crane-2C (A-4), %	Morita (A-5), %	M & W (A-6), %	Lin (A-7), %	S & D (A-8), %
1-a	f = 10–15 GHz	1.	159	100	51	66	83	68	32*	39†
	Rain rate:	0.1	56	60	58	53*	71	53*	61	54
	CCIR zone	0.01	42*	46	50	45†	63	47	61	52
		0.001	66†	75	85	71	108	60*	99	81
1-b	f = 10–15 GHz	1.	257	151	74	...	116	71	62*	70†
	Rain rate:	0.1	62†	64	64	...	77	57*	62†	63
	measured	0.01	45†	47	43*	...	70	80	56	50
		0.001	51†	61	51†	...	153	89	60	48*
2-a	f = 10–15 GHz	1.	122	80	52	54	88	61	29*	35†
	Rain rate:	0.1	49†	62	64	56	84	40*	69	61
	CCIR zone	0.01	39	42	30†	31	56	27*	53	39
	El ≤ 20°	0.001	11*	16	17	23	47	13†	24	17
2-b	f = 10–15 GHz	1.	72	55	24	...	23	16*	22†	23
	Rain rate:	0.1	54†	70	68	...	52*	65	56	63
	measured	0.01	67	72	49	...	6*	7†	62	73
	El ≤ 20°	0.001	...	...	...	...	...	...	...	...
3-a	f = 10–15 GHz	1.	169	106	46	70	80	66	33*	40†
	Rain rate:	0.1	57	59	58	54†	70	54†	61	53*
	CCIR zone	0.01	42*	46	51	45†	62	49	62	53
	El > 20°	0.001	67†	77	86	72	105	61*	101	83
3-b	f = 10–15 GHz	1.	282	163	80	...	129	78	68*	77†
	Rain rate:	0.1	62†	62†	64	...	80	56*	62†	63
	measured	0.01	45†	46	43*	...	67	84	56	49
	El > 20°	0.001	51†	61	51†	...	153	89	60	48*
4-a	f = 15–20 GHz	1.	208	131	69	108	86	77	54*	61†
	Rain rate:	0.1	41	40	36*	36*	42	39	37	36*
	CCIR zone	0.01	32*	33†	38	28	49	41	44	38
		0.001	52*	58	84	57†	61	87	66	80
4-b	f = 15–20 GHz	1.	410	234	112	...	146	142	96*	110†
	Rain rate:	0.1	60	58	25†	...	60	60	26	24*
	measured	0.01	50	49†	45*	...	66	59	62	49†
		0.001	37	38	38†	...	160	164	7*	25

*Best values.
†Second best values.

2. As for the standard deviation, one of the CCIR methods (A-1), Misme and Waldteufel's method (A-6), and Lin's method (A-7), are relatively superior.

3. No significant difference is observed when rainfall intensity is given by either experimental values or assigned values from the CCIR rain climatic zones. An accurate prediction is therefore not necessarily guaranteed because measured rain rate data are used.

4. For methods other than the CCIR methods (A-3 to A-8), there is a tendency to overestimate the attenuation for a smaller fraction of time, and underestimate it for a larger fraction of time.

5. Overall, the CCIR methods (A-1 and A-2) give a more accurate prediction than the other methods.

Focusing on the CCIR method (A-2), the mean discrepancy for 0.01% of the time using the CCIR zone rain rate is shown in Table 3. Values in the table are given for the three areas of E, K, and M where more than 10 measurements are available. From this table, the following can be seen:

6. As for the CCIR method (A-2), we can see the

TABLE 3. Mean Errors of the CCIR Method (A-2) for Three Kinds of CCIR Rain Climatic Zone

	Region		
CCIR Climatic Zone	E	K	M
$R_{0.01}$, mm/h	22	42	63
Mean error ΔX, %	−13	1	14
Number of data	24	38	16

trend that calculated values are likely to be underestimated for regions where rainfall intensity is low (region E), and conversely, overestimated for regions where rainfall intensity is relatively high (region M).

Moreover, apart from the fact that a good prediction method should give a high accuracy of prediction, it is also said that the simplicity of the model, physical significance and flexibility are also of prime importance [*Fedi*, 1981]. Table 4 compares each of the various models from this viewpoint (the evaluation may however be influenced to some extent by the authors' subjective impressions). From this table, the following can be seen:

7. The CCIR methods are also the best from the viewpoint of ease of use. These methods consist only of simple equations, and in addition, the rain attenuation for any time percentage can be calculated by using only 0.01% rain rate. In contrast, other methods require input of the rainfall rate for each fraction of time, or one set of rain rate data with a different fraction of time. This demonstrates the superiority of the CCIR methods.

TABLE 4. Evaluation From the Point of Convenience

	Simplicity	Physical Meaning	Flexibility	Mark*
A-1 CCIR MOD I	3	1	2	13
A-2 CCIR MOD F	3	1	2	13
A-3 Crane-G	2	2	1	11
A-4 Crane-2C	1	3	1	10
A-5 Morita	2	2	1	11
A-6 M & W	0	3	1	7
A-7 Lin	2	1	2	10
A-8 S & D	2	2	1	11

*Simplicity, ×3; physical meaning, ×2; flexibility, ×1. Full mark is 18.

3. AN IMPROVED PREDICTION METHOD

In the previous section, we have shown that, at the present time, the CCIR methods are superior to the other methods, insofar as both prediction accuracy at frequencies from 10 to 20 GHz and ease of use are concerned. In this section, we will attempt to devise an improved method with greater accuracy reflecting the result of evaluations performed.

Many prediction methods, including the CCIR methods, depend on the following basic relation:

$$A = kR^{\alpha}L_e \quad \text{dB} \tag{1}$$

where kR^{α} is the specific attenuation (decibels per kilometer) for a spatially uniform rainfall intensity R (millimeters per hour) and L_e is the effective path length in kilometers. The effective path length is determined by getting information regarding the vertical and horizontal extent of rain volume (we will refer to the horizontal extent hereafter as the characteristic length for the sake of convenience).

We therefore consider an improved method using characteristic length so as to minimize prediction error.

In the CCIR model, effective path length is given by

$$L_e = L_s/(1 + L_s \cos\theta/L_0) \tag{2}$$

In this equation, L_s is the slant path length determined by the effective rainfall height and the elevation θ, and L_0 is the characteristic length of a rain cell. In the CCIR model, L_0 is given by a fixed value of 22.5 km.

If we limit our consideration to a given area, the size of the rainfall area is generally smaller when the rainfall becomes very heavy, as in the case of convective rain (corresponding, for example, to rains for 0.01% to 0.001% of the time), than when it is weak (e.g., 0.1%). However, regarding the characteristic length, namely, the size of the rain area for the 0.01% rain rate, there are not necessarily any well-defined differences among areas with different climates. As we described in the previous section, therefore, the attenuation can be predicted with a fairly high degree of precision even if the characteristic length is taken to be constant, as in the CCIR model.

On the other hand, according to the results of the analysis in case 6 of the previous section, the characteristic length seems to have a slight dependence on the 0.01% rain rate itself. Better accuracy may thus be obtained by considering the characteristic length to be smaller for heavy rain areas.

We now assume the relation:

$$L_0 = a \exp(-bR_{0.01}) \quad (3)$$

where L_0 is the characteristic length for the 0.01% rain rate, $R_{0.01}$.

Table 5 shows the mean value and standard deviation of prediction errors for case 1-a in Table 2, as a function of the parameters a and b in equation (3). The values of a and b have been chosen such that the characteristic length is approximately 20 km when the rainfall rate is about 40 mm/h. In Table 5, the case where $a = 22.5$, and $b = 0$ corresponds to CCIR model A-2 itself.

From Table 5, it can be seen that the best values for the mean are obtained for $a = 35$, $b = 0.015$, while better values for standard deviation are obtained for $a = 40$, $b = 0.02$. In the latter case, however, mean error increases when the time percentage factor becomes larger. In (3) therefore we choose $a = 35$ and $b = 0.015$.

Table 6 shows the prediction accuracy of the improved method stated above. (A step-by-step calculation method is presented in the appendix.) For the purpose of comparison with Table 2, the asterisks and daggers have been used to denote the new best and new second best values among the existing and proposed methods. As can be seen from this table, the proposed method gives predicted values which are considerably better than those of other methods, and, particularly, the mean values of errors can be significantly reduced. As for the CCIR method A-2, there is a trend for the predicted values to be lower than the experimental values for rainless regions, and to be larger for heavy rain regions. In the proposed method introducing the characteristic length L_0 as a function of the 0.01% rain rate, it is possible to eliminate this trend.

As a reference, Figure 1 shows a scattergram of experimental values and corresponding predicted values calculated by the proposed method for case a and case b.

TABLE 6. Results of Evaluation for the Proposed Method

Case	Condition	Time Rate, %	$\overline{\Delta X}$, %	$\sigma_{\Delta x}$, %
1-a	f = 10–15 GHz	1.	−4*	93
	Rain rate:	0.1	0*	51*
	CCIR zone	0.01	0*	40*
		0.001	3*	63†
1-b	f = 10–15 GHz	1.	−2*	135
	Rain rate:	0.1	3*	54*
	measured	0.01	8*	37*
		0.001	7*	53
2-a	f = 10–15 GHz	1.	−13	68
	Rain rate:	0.1	−12	35*
	CCIR zone	0.01	10*	27*
	El ≤ 20°	0.001	41†	15
2-b	f = 10–15 GHz	1.	−12	33
	Rain rate:	0.1	−11	45*
	measured	0.01	22*	54
	El ≤ 20°	0.001	...	...
3-a	f = 10–15 GHz	1.	3*	98
	Rain rate:	0.1	6	52*
	CCIR zone	0.01	−2*	41*
	El > 20°	0.001	1*	64†
3-b	f = 10–15 GHz	1.	13*	146
	Rain rate:	0.1	15	53*
	measured	0.01	5*	37*
	El > 20	0.001	7*	53
4-a	f = 15–20 GHz	1.	32	115
	Rain rate:	0.1	−5	39
	CCIR zone	0.01	−7	32*
		0.001	21*	58
4-b	f = 15–20 GHz	1.	35	195
	Rain rate:	0.1	9	51
	measured	0.01	−2*	37*
		0.001	−21*	36

*Best values.
†Second best values.

TABLE 5. Prediction Errors of the Proposed Method for Case 1-a as a Function of a and b of Equation (3)

	Time Rate, %	a = 22.5, b = 0	a = 30, b = 0.01	a = 35, b = 0.015	a = 40, b = 0.02
ΔX, %	1.	12	1	−4	−10
	0.1	13	4	0	−5
	0.01	6	2	0	−3
	0.001	7	5	3	2
$\sigma\Delta x$, %	1.	100	95	93	90
	0.1	60	54	51	50
	0.01	46	42	40	38
	0.001	75	68	63	58

4. CONCLUSION

An evaluation of errors associated with eight existing methods, including those of the CCIR, for pre-

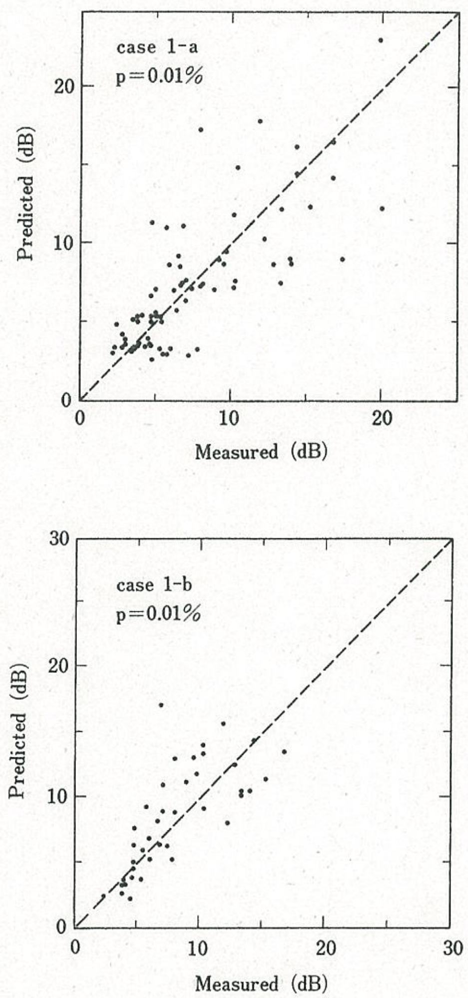

Fig. 1. Scattergram of predicted and measured attenuations for 0.01% of the time. (*a*) Case 1-a; (*b*) case 1-b.

dicting rain attenuation on oblique (Earth-to-space) propagation paths was made, based on 124 sets of data which have so far been reported for frequencies of 10–20 GHz. The results showed that the CCIR methods gave relatively high accuracy, although in this respect there was not such a great difference from other methods.

As the CCIR methods are very easy to use, we used them as a basis to attempt to improve the accuracy of prediction. The CCIR methods predict values higher than those of the experimental data for areas with heavy rainfall, and they tend to give lower values than the data for areas with low rainfall. The method proposed here includes a rain size parameter as a function of the rain rate for 0.01% of the time so as to minimize the prediction error, and therefore the method can eliminate the above shortcoming of the CCIR methods. It was verified that the method thus obtained gives the best precision, at the present time, for predicting rain attenuation on Earth-to-space propagation paths at 10–20 GHz.

Most prediction methods, including the proposed one, assume a single volume for falling rain, but actually there must be two types of rainfall: convective rain (cell), and stratified rain (debris). The Crane's two-component mode A-4, wherein these two types are mixed together, is therefore quite persuasive. The fact that the Crane's two-component model does not necessarily give better results than the other methods may be due to the difficulty of assigning rainfall parameters (e.g., probabilities of occurrence and mean rainfalls, for cell and debris). In other words, it is probably largely due to the difficulty of determining accurate parameters.

Further, as most of the data obtained up to now consist of measurements in middle latitude regions at relatively high elevation angles, the prediction of attenuation for propagation paths with low elevations or in equatorial regions with heavy rainfall, has not yet been fully evaluated. This task remains to be accomplished when sufficient new data beome available.

APPENDIX: STEP-BY-STEP-CALCULATION PROCEDURE OF PROPOSED METHOD

Step 1. Identify the one-minute rain rate of the site for 0.01% of the time, $R_{0.01}$ (mm/h), from measurements, otherwise CCIR rain climatic zone data.

Step 2. Calculate the specific attenuation, A_s (dB/km) given by

$$A_s = kR_{0.01}^{\alpha}$$

k, α are given in Rep. 721 of the CCIR.

Step 3. Calculate the slant path length, L_s, as a function of elevation angle, θ, and altitude of the site, H_s,

$$L_s = (H - H_s)/\sin\theta \qquad \theta \gtrsim 10^\circ$$

where H is effective rain height given by

$$H = 4 \text{ (km)} \qquad 0^\circ \le \phi \le 36^\circ$$

$$H = 4 - 0.075(\phi - 36) \qquad \phi > 36^\circ$$

and ϕ is latitude of the site. When calculating

$\theta < 10°$, more exact formulation should be employed (CCIR 564-2).

Step 4. Calculate the characteristic length of the rain size for 0.01% of the time, L_0,

$$L_0 = a \exp(-bR_{0.01})$$

where $a = 35$ and $b = 0.015$.

Step 5. Calculate the effective path length, L_e,

$$L_e = L_s/(1 + L_s \cos\theta/L_0)$$

Step 6. Calculate the rain attenuation for 0.01% of the time, $A_{0.01}$ (decibels),

$$A_{0.01} = A_s L_e$$

Step 7. Calculate the rain attenuation for p% of the time, A_p (decibels),

$$A_p = 0.12 A_{0.01} p^{-(0.546 + 0.043 \log p)}$$

for $0.001 \leq p \leq 1$.

Acknowledgments. We would like to express our deep appreciation to K. Nosaka, T. Muratani, T. Shiokawa and K. Yasukawa of KDD for their encouragement and valuable cooperation to this study.

REFERENCES

Allnutt, J. E., Prediction of micro-wave slant-path attenuation from point rainfall-rate measurements, *Electron. Lett., 23rd, 13*(13), 376, 1977.

CCIR Rep. 563-2, Radio meteorological data, SG5, International Telecommunications Union, Geneva, 1982.

CCIR Rep. 564-2 (MOD I), Propagation data required for space telecommunication systems, SG-5, International Telecommunications Union, Geneva, 1984.

CCIR, Data banks used for testing prediction methods in section E, F and G of volume V, Doc. 5/378 (Rev. 1)-E, WG 5-E, International Telecommunications Union, Geneva, Oct. 1985.

CCIR Rep. 564-2 (MOD F), Propagation data required for space telecommunication systems, SG-5, International Telecommunications Union, Geneva, 1986.

Crane, R. K., Prediction of attenuation by rain, *IEEE Trans. Commun., COM-28, 9*, 1717–1733, 1980.

Crane, R. K., Comparative evaluation of several rain attenuation prediction models, *Radio Sci., 20*, 843–863, 1985*a*.

Crane, R. K., Evaluation of global and CCIR models for estimation of rain rate statistics, *Radio Sci., 20*, 865–879, 1985*b*.

Dintelman, F., Results obtained from attenuation measurements of the Deutsche Bundespost OTS-propagation experiment, paper presented at Commission F Open Symposium, URSI, Louvain, Belgium, 1983.

Fedi, F., Prediction of attenuation due to rainfall on terrestrial links, *Radio Sci., 16*, 731–743, 1981.

Lin, S. H., Empirical rain attenuation model for earth-to-space paths, *IEEE Trans. Commun., COM-27*(5), 812–817, 1979.

Lin, S. H., H. J. Bergman, and M. V. Pursley, Rain attenuation on Earth-satellite-paths: Summary of 19-year experiments and studies, *Bell Syst. Tech. J., 59*, 183–228, 1980.

Misme, P., and P. Waldteufel, A model for attenuation by precipitation on a microwave Earth-to-space link, *Radio Sci., 15*, 655–665, 1980.

Morita, K., Estimation methods for propagation characteristics on Earth-to-sace links in microwave and millimeter wavebands, *Rev. ECL NTT Jpn., 28*, 459–471, 1980.

Rogers, D. V., Diversity measurements of 11.6-GHz rain attenuation at Etam and Lenox, West Virginia, *COMSAT Tech. Rev., 9*, 243–254, 1979.

Rogers, D. V., and G. Hyde, Statistics of 11.6 GHz atmospheric attenuation and rainrate observed in diverse climates, *COMSAT Lab. Tech. Memo., CL-22-78*, 1, 1978.

Rucker, F., Simultaneous propagation measurements in the 12-GHz band on the SIRIO and OTS satellite links, paper presented at Commission F Open Symposium, URSI, Lennoxville, Canada, May 1980.

Rustako, A. J., Jr., An earth-space propagation measurement at Crawford Hill using the 12-GHz CTS satellite beacon, *Bell Syst. Tech. J., 57*, 1431–1448, 1978.

Satoh, K., Y. Hosoya, and S. Kato, Rain attenuation characteristics on slant paths in 20 and 30 GHz bands, *Trans. Inst. Electron. Commun, Eng., Jpn., E-61*(9), 697–703, 1978.

Stutzman, W. L., and W. K. Dishman, A simple model for the estimation of rain-induced attenuation along Earth-to-space paths at millimeter wavelengths, *Radio Sci., 17*, 1465–1476, 1982.

Wilson, R. B., and W. L. Mammel, Results from a three radiometer path diversity experiment, Propagation of Radio Waves at Frequencies Above 10 GHz, *Inst. Elec. Eng. Publ., 98*, 23–27, 1973.

Yamada, M., O. Furuta, H. Yokoi, and A. Ogawa, Rain attenuation measurement by dual-frequency rader, *Trans. Inst. Electron. Commun. Eng. Jpn, J64-B*(9), 947–954, 1981.

Yasukawa, K., and M. Yamada, The 11.9-GHz rain attenuation and site diversity effect on the Earth-space paths of low elevation angles, *Radio Sci., 20*, 1565–1579, 1985.

B. Arbesser-Rastburg, Antennas and Propagation, R & D, INTELSAT, 3400 International Drive, N.W., Washington, DC 20008.

Y. Karasawa, M. Yamada, and M. Yasunaga, Research and Development Laboratories, KDD, 2-1-23 Nakameguro, Meguro-ku, Tokyo 153, Japan.